*Ann. occup. Hyg.*, Vol. 46, No. 6, pp. 511–522, 2002
Published by Oxford University Press
DOI: 10.1093/annhyg/mef063

# Thoracic Size-selection of Fibres: Dependence of Penetration on Fibre Length for Five Thoracic Sampler Types

**ANDREW D. MAYNARD***

*Health and Safety Laboratory, Health & Safety Executive, Broad Lane, Sheffield S3 7HQ, UK*

Received 1 October 2001; in final form 7 February 2002

**It has been suggested that the non-size-selective sampling methods currently used for fibrous aerosols potentially lead to the presence of large compact particles, agglomerates and fibre clumps in samples, which in turn reduce the accuracy and precision of the manual fibre counting techniques employed to analyse samples. The use of thoracic size-selective samplers has been proposed as an alternative, leading to the prevention of large particles reaching the collection substrate while at the same time bringing fibre sampling into line with general occupational aerosol sampling methodologies. Thoracic samplers should give good agreement with current sampling methods under ideal conditions based on aerodynamic fibre properties. However, the effect of fibre length on sampling efficiency is not known. The sampling efficiency of five thoracic samplers was therefore measured as a function of fibre length for respirable fibres between 10 and 60 μm long. These included the commercially available GK2.69 cyclone and the CATHIA sampler, the IOM thoracic sampler, a modified version of the SIMPEDS cyclone and a modified version of the IOM inhalable sampler. Length-monodisperse fibres were generated using a dielectrophoretic fibre classifier and sampler penetration was measured as a function of fibre length. No length-dependent sampling effects were observed for the CATHIA, GK2.69, modified SIMPEDS and modified IOM inhalable samplers for fibres <60 μm. Data for the IOM thoracic sampler showed a significant trend of reducing sampling efficiency for fibres >30 μm. Overall, the laboratory results indicated that the five sampler types are likely to perform as well as or better than the currently used 25 mm cowled sampler in the field.**

*Keywords:* fibre; size-selective aerosol sampling; sampler penetration; fibre length classification

## INTRODUCTION

Recent years have seen the formulation and adoption of harmonized size-selective aerosol sampling criteria for occupational exposure assessment (Comité Européen de Normalisation, 1993; International Standards Organization, 1995; American Conference of Government Industrial Hygienists, 1998). The resulting conventions define particle penetration into the respiratory system and to the thoracic and alveolar regions, thus allowing exposure limits to be based on potential exposure to the most sensitive regions of the lungs. Although size-selective occupational aerosol sampling has been widely adopted internationally, fibrous aerosols form a notable exception. The toxicity of respirable fibrous particles, such as man-made mineral fibres and asbestos fibres, is associated with particle shape and thus, historically, the approach to assessing exposure has been different from compact particles. Fibrous aerosols are generally sampled using a 25 mm diameter 'cowled' sampler with negligible particle size selectivity below 20 μm aerodynamic diameter onto a membrane filter. Fibres collected on the filter are imaged using either electron microscopy or phase contrast optical microscopy and are manually counted using selection rules based on their diameter and aspect ratio (World Health Organization, 1997).

The accuracy and precision of airborne fibre concentration measurements is notoriously poor. During sample analysis only fibres that are able to reach the alveolar region of the lungs, respirable

*Author to whom correspondence should be addressed. Current address: US Department of Health and Human Services, Public Health Service, Centers for Disease Control and Prevention, National Institute for Occupational Safety and Health, Division of Applied Research and Technology, 4676 Columbia Parkway, Cincinnati, OH 45226, USA.

fibres, are counted. Where fibres are present in the sample as compact agglomerates with other fibres or particles they are not counted (World Health Organization, 1997). However, the likelihood of particle overlap occurring on the sampling substrate at high fibre concentrations or high compact particle concentrations leads to the possibility of this counting rule leading to the actual respirable fibre concentration being substantially underestimated. The interpretation of samples containing large numbers of clumps and compact particles is also suspected of leading to an increased number of operator-based decisions during manual counting, leading to reduced precision between repeat analyses. It has been proposed that exclusion of such particles from samples would potentially lead to greater analysis precision in some cases (Lippmann, 1994a,b; World Health Organization, 1997). The introduction of size-selective sampling to airborne fibres would allow a reduction in non-respirable clumps and compact particles within samples, potentially leading to increased accuracy and precision within sample analyses. It would also allow fibre sampling to be brought into line with standard occupational aerosol sampling methods.

Although the application of the respirable convention would seem an obvious solution to size-selective fibre sampling, Baron (1996) has shown that this would lead to the exclusion of some fibres currently considered countable. As any new sampling method will be required to give the same results as current methods under ideal conditions, the particle size selectivity criteria used would need to allow all fibres currently considered countable onto the collection substrate. By using the thoracic convention, this condition is met, while excluding particles larger than ~10 μm aerodynamic diameter that could potentially confound sample analysis (Baron, 1996). The use of thoracic samplers for fibre sampling will only be comparable with current techniques if fibre size selectivity is based on aerodynamic diameter alone. Current aerosol sampler characterization methods use spherical or compact particles that provide penetration or collection efficiency measurements as a function of aerodynamic diameter, but provide no information on how particle shape influences particle interception within the device, which may be important for fibres. It is thus possible that a thoracic sampler shown to perform well with spherical particles will not show the same behaviour when challenged with high aspect ratio fibrous particles.

The sampling characteristics of a number of thoracic samplers has previously been measured and a number of them shown to agree well with the thoracic sampling convention (Maynard, 1999). This paper presents research into the sampling efficiency of these thoracic samplers with fibrous aerosols. Such a characterization is not trivial and a number of assumptions have been necessary to allow a series of valid measurements. The fundamental assumption has been that the distinguishing factor between the penetration of compact and fibrous particles with the same aerodynamic diameter is fibre length alone. If this assumption is valid, then measured differences between the penetration of aerodynamically similar fibres and compact particles will be indicative of sampler performance in the field.

The method selected to measure fibre penetration through the thoracic samplers was to use length-monodisperse fibrous aerosols. Details of a device developed to generate an aerosol of glass fibre particles within very narrow length constraints have been published previously (Deye *et al.*, 1999). This fibre classifier was further developed to provide a suitable fibrous aerosol test system. Penetration measurements were made with each of the thoracic samplers using single length man-made mineral fibres with aerodynamic diameters smaller than ~5 μm.

## SAMPLERS

Five thoracic sampler types previously characterized using spherical particles (Maynard, 1999) were selected for testing.

The GK 2.69 cyclone (BGI Inc., USA) was developed through research into a family of tangential flow cyclones (Kenny and Gussman, 1997). It has been designed as a dual fraction sampler, operating as a respirable sampler at 4.2 l/min and a thoracic sampler at 1.6 l/min. Aerosol is sampled onto a 37 mm filter which is attached to the cyclone via a standard 37 mm filter cassette. In this investigation an additional filter cassette ring was placed between the vortex finder and the aerosol outlet to aid particle dispersion across the width of the filter holder (necessary to give an even dispersion when sampling fibres onto filters).

The CATHIA sampler (ARELCO, France) is a variant of the CIP-10 sampler designed for stand-alone use (Fabriès *et al.*, 1998). It is configurable with a range of different heads, but was used with the thoracic head in this instance. When used with the thoracic head the sampler is operated at 7 l/min. Size-selected aerosol is sampled through a flow column 32 mm in diameter and 110 mm long, designed to allow the aerosol to disperse across the full width of the volume, before deposition onto a 25 mm diameter filter.

Recent research at the National Institute of Working Life (NIWL) in Sweden and the Lund Institute of Technology has led to a modified version of the SIMPEDS or Higgins–Dewell respirable cyclone to give a thoracic penetration curve at a flow rate of 0.8 l/min. Aerosol is collected onto a 25 mm filter separated from the cyclone outlet by 33 mm to allow a homogeneous particle distribution across the collection substrate.

The IOM foam thoracic sampler has arisen from research at the Institute of Occupational Medicine (IOM) in Edinburgh into inhalable inlets and foam aerosol separators (Aitken *et al.*, 1993). A 30 pores per inch (p.p.i.) foam, 29 mm in diameter and 24 mm deep, is placed behind an inlet identical to that used on the IOM inhalable sampler and the sampler is operated at 2 l/min to give a thoracic cut.

Following research into the use of porous polyurethane foam as a size-selective aerosol preseparator (Vincent *et al.*, 1993; Kenny and Stancliffe, 1997), Maynard (1999) showed that the inclusion of a porous polyurethane foam plug of 45 p.p.i., 10 mm deep and 17.5 mm in diameter, in an IOM inhalable sampler inlet (SKC Inc., USA) gives an acceptable thoracic cut at 2 l/min. This sampler, referred to as the modified IOM inhalable sampler, was also included in these tests (a commercial version of the IOM sampling head using a similar approach to give a thoracic cut is marketed by SKC Inc., USA).

## FIBRE CLASSIFICATION

The study of how aerosol samplers respond to fibres has been severely limited in the past by the lack of appropriate test aerosols with narrow length and diameter ranges. Methods previously employed to generate length-monodisperse fibrous aerosols have included cutting continuous fibres into well-defined lengths using either a microtome or laser (Lipowicz and Yeh, 1989) or using silicon wafer lithography techniques to micromachine fibres of specific lengths and aspect ratios (Kaye *et al.*, 1992; Chen *et al.*, 1993). However, these techniques have proved to produce particles in insufficient quantities or of insufficient quality for sampler penetration testing. An alternative approach is to separate fibres of the desired characteristics from a polydisperse aerosol. Lipowicz and Yeh (1989) calculated that by using dielectrophoretic motion in a non-uniform electric field, airborne fibres as short as 10 μm could be separated from a length-polydisperse aerosol. Based on these calculations Baron *et al.* (1994) constructed a dielectrophoretic fibre separator that demonstrated the applicability of this principle. Further research led to the development of a differential classifier capable of outputting length-monodisperse fibrous aerosols (Baron *et al.*, 1998; Deye *et al.*, 1999).

Measurements of thoracic sampler penetration as a function of fibre length were made using fibres generated using the differential dielectrophoretic classifier described by Deye *et al.* (1999). For this investigation modifications were made to the flow control and voltage systems to allow a degree of automation. However, the classifier itself was left unmodified.

Figure 1 shows a schematic of the classifier in the configuration used for this investigation. Sampled fibres are initially restrained within an annular airflow between two clean sheath airflows, the outer and inner sheath flows. Fibres are then passed through an annulus defined by two concentric electrodes, between which an alternating high voltage is applied. Conducting fibres become polarized in the electric field and move along the field gradient towards the inner electrode through the process of dielectrophoresis. The dielectrophoretic velocity of the particles is proportional to the applied root mean square voltage and fibre length. By removing a small annulus of airflow at the base of the inner electrode, fibres travelling at a specific dielectrophoretic velocity, and thus having a specific length, are removed from the aerosol. Characteristic classified fibre length is inversely proportional to the applied voltage and thus, by altering the voltage, well-defined length-monodisperse fibres may be removed from a length-polydisperse aerosol. Although the classification mechanism depends on fibres being conductive, in practice the presence of a slightly conductive coating is sufficient to lead to polarization in the electric field. For non-conductive glass fibre this is effectively achieved by maintaining a relative humidity >60% within the classifier, the resulting thin layer of adsorbed water molecules on the fibres providing sufficient conductivity.

In the classifier configuration used for this study the inner and outer sheath flows to the classifier, together with the sample and dump flows, were regulated using digital mass flow controllers (Brooks, Germany). Voltage applied to the inner electrode of the classifier was provided by a proprietary programmable high voltage square wave generator. Length-monodisperse fibres leaving the classifier in the sample flow were either counted using an aerodynamic particle sizer (APS 3310; TSI, USA) or were collected onto a membrane filter for analysis in a scanning electron microscope (SEM). The temperature and humidity of the flow within the classifier were constantly monitored, as was the pressure drop across the inlet and the dump flow outlet. Aerosol was moved through the classifier using two diaphragm pumps in push–pull mode to allow air re-circulation and to minimize pressure drops within the device. Flow pulsations arising from the pumps were damped using a combination of expansion volumes and flow restrictors and the residual pulsation level monitored using an electret microphone at the classifier inlet. All operations were controlled and monitored using proprietary LabView (National Instruments Inc.) routines on a PC.

Within the context of the sampler penetration measurements it was important to maximize the throughput of classified fibres while keeping the fibre length distribution as narrow as possible. Classifier throughput can be increased by increasing the relative flow within the sampled aerosol annulus. However, as throughput increases, the length distri-

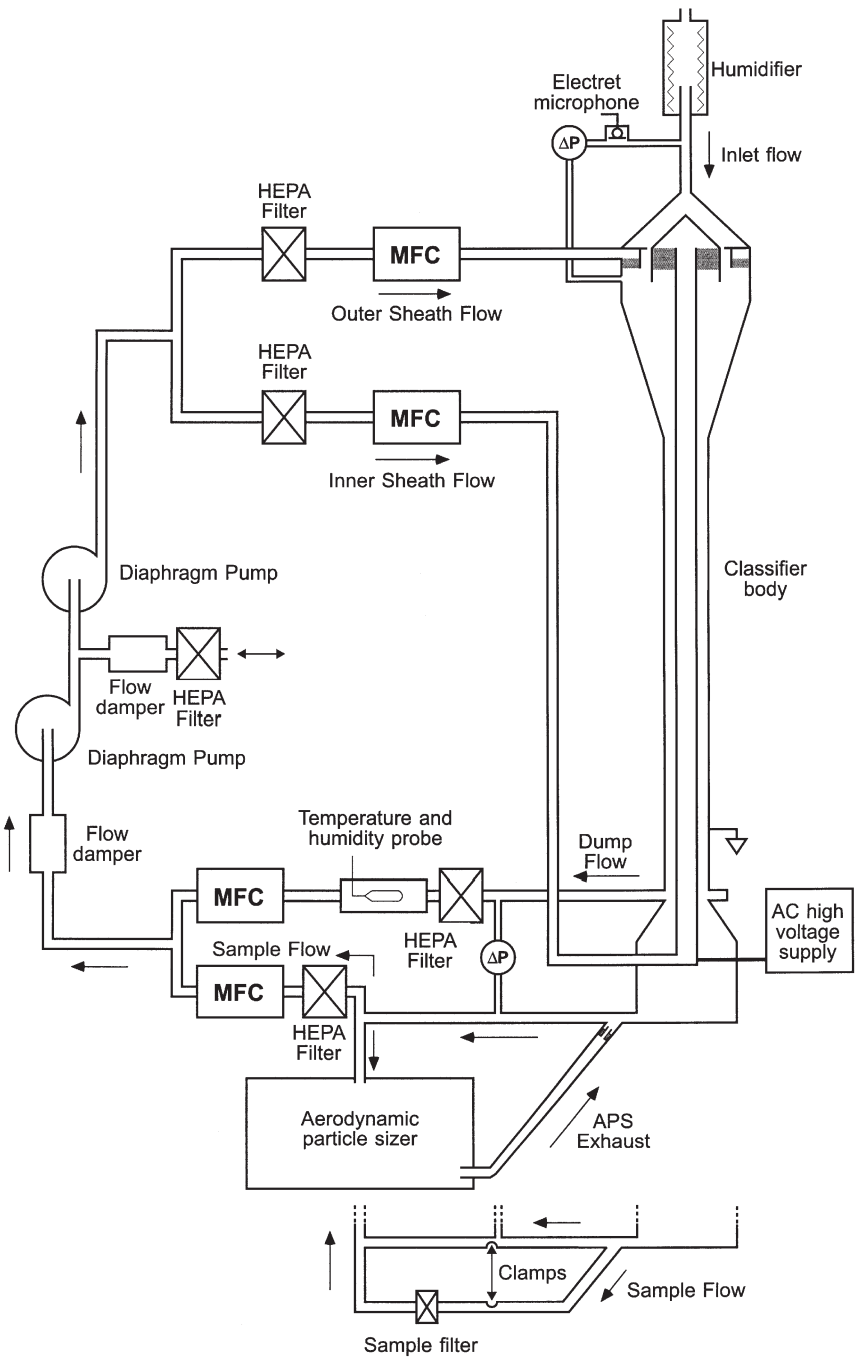


**Fig. 1.** Schematic of the fibre classifier flow and control system.

bution of the classified fibres widens. The length distribution is further broadened if turbulent mixing occurs between the aerosol and sheath flows. An effective method of measuring the effects of sampling flow rate and turbulent mixing on the width of the classified fibre length distribution is to measure the containment of the annular aerosol flow between the inner and outer sheath flows. Containment of the aerosol flow within the fibre classifier was measured using the split flow method described by Deye *et al.* (1999). The sample flow is drawn from the radial centre of the cylinder defined by the outer electrode. If this sample flow is increased, it takes an increasing radial share of the flow through the classifier. In the hypothetical situation of no mixing between the sheath flows and the aerosol flow, the particle count in the sample flow would remain zero until the sample flow exceeded the inner sheath flow (say

$Q_{S1}$). Then further increases in sample flow would produce a linear increase in the particle count, until the sample flow exceeded the total of inner sheath flow and aerosol flow ($Q_{S1} + Q_{aerosol}$). In this hypothetical situation the particle count would rise as the diagonal of the dotted rectangle in Fig. 2. Still under the hypothetical situation of no flow mixing, once the flow exceeds $Q_{S1} + Q_{aerosol}$, all the aerosol would be in the sample flow and the particle count would remain constant.

From the observed cumulative particle count the distribution of particle concentration across the radius of the cylinder can be calculated. This gives a 'radial particle concentration', where the particle concentration is the number of particles per unit flow as a function of radial position. For the hypothetical case of no mixing, radial particle concentration plotted against sample flow will result in a top-hat function (Fig. 2).

Containment of the inlet flow was measured by introducing an aerosol of 1.0 μm diameter monodisperse polystyrene spheres (PSL) to this flow, while keeping the total flow through the classifier at 5 l/min. Aerosol radial profiles were collected by programming a set sequence of sample/dump flow splits within LabView and using the same program to measure particle concentration in the sample flow with the APS at each sample flow value. Four classifier flow configurations were investigated to enable the best balance between classified fibre throughput and fibre length.

1. Sheath and inlet flows were set to give equal air velocities where the flows combine. Turbulent mixing between the flows would be minimized in this configuration, but a broad length distribution would be expected due to the relatively large inlet flow rate necessary. Under these conditions the inlet flow was set to 1.5 l/min and the two sheath flows to 1.75 l/min.
2. The inlet flow rate was set to 0.5 l/min to reduce the width of the fibre length distribution, while the inner sheath flow velocity was matched with the inlet flow velocity to minimize turbulent mixing, giving an inner sheath flow of 0.58 l/min and an outer sheath flow of 3.92 l/min.
3. The inlet flow rate was set to 0.5 l/min to give a narrow fibre length distribution, while the outer sheath flow velocity was matched with the inlet flow velocity to minimize turbulent mixing, giving an inner sheath flow of 3.92 l/min and an outer sheath flow of 0.58 l/min.
4. The inlet flow was set to 0.5 l/min to give a narrow fibre length distribution, while the sheath flows were set to equal flow rates of 2.25 l/min. In this configuration the possibility existed for limited turbulent mixing between the aerosol and sheath flows, although it was considered likely that overall turbulent mixing would be less than in cases 2 and 3 above given the smaller differences in relative flow velocities.

Figure 2 shows the normalized cumulative and differential spherical aerosol concentrations as a function of sample flow rate, together with the theoretical differential flow rate assuming no aerosol or flow mixing. Figure 2a shows the half width of the inlet flow annulus to be approximately equal to the theoretical profile for equal sheath and inlet velocities. However, in this configuration the unclassified aerosol is contained in a sizeable fraction of the total flow, leading to poor fibre length selectivity. The profile also indicates slightly more mixing with the inner sheath flow, shown by the profile tail at low sample flow rates. Figure 2b shows the flow profile when matching the velocity of the inner sheath flow with the inlet flow. Significant mixing is shown across the width of the inner sheath flow, as well as a relatively high degree of mixing with the outer sheath flow. Figure 2c shows the flow profile when matching the inlet flow and outer sheath flow velocities. The profile deviates significantly from the theoretical profile, indicating severe mixing with both sheath flows. Finally, Fig. 2d shows the flow profile for equal sheath flow rates and a low inlet flow (for high resolution fibre length differentiation). The half width of the profile is ~30% wider than the theoretical profile, indicating a greater degree of mixing than in Fig. 2a. However, the results indicate that mixing due to disparate flow velocities between the inlet and sheath flows is not severe. In this configuration the inlet aerosol is still contained within a sufficiently narrow annulus to classify fibres with a narrow length distribution. Subsequent sampler penetration measurements were made operating the classifier under these conditions.

The fibre classifier was calibrated using a fibrous aerosol generated from Schuller 108A bulk glass-fibre. The glass fibre was initially ground in a rotary mill and then finely ground in a micronizing mill to form a powder with a significant number concentration of fibres shorter than 50 μm. This was subsequently aerosolized using a fluidized bed generator (Model 3400; TSI Inc., USA). The aerosol was brought to charge equilibrium using a $^{85}Kr$ source on the inlet of the fibre classifier. For calibration purposes, classified fibres were collected on a polycarbonate membrane filter (Fig. 1). Length analysis of classified fibres in the SEM was used to measure fibre length as a function of applied voltage. An electron micrograph of typical classified fibres is shown in Fig. 3, while Fig. 4 plots normalized measured length distribution as a function of applied voltage. At all times the classifier was operated at a sampling flow rate of 0.5 l/min, sheath flow rates of 2.25 l/min and a classified fibre output flow rate of 0.5 l/min. Table 1 gives the measured fibre length distribution

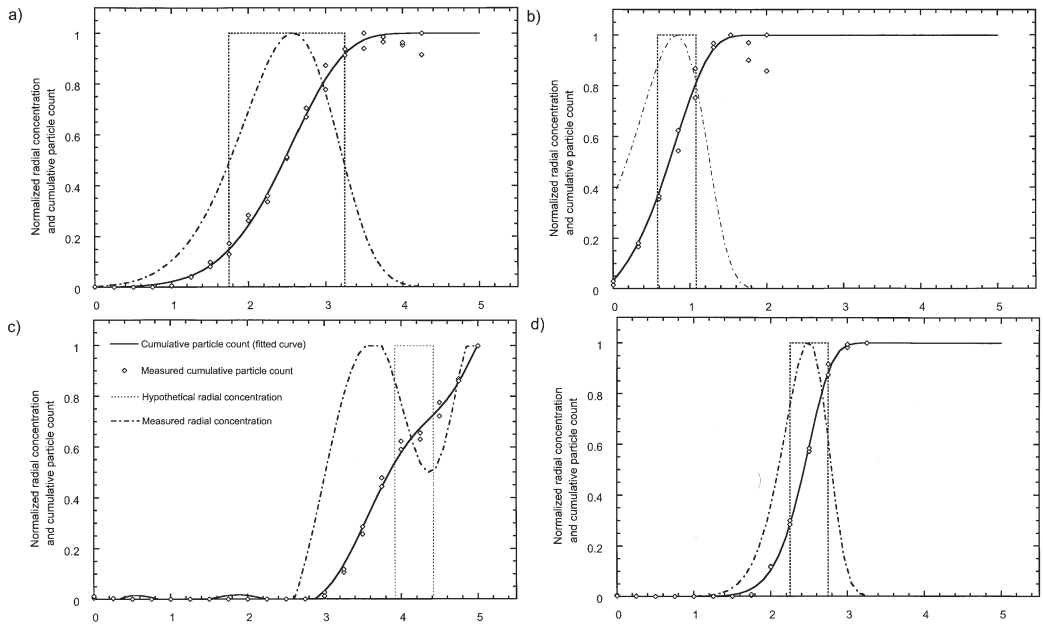


**Fig. 2.** Predicted and measured radial aerosol concentrations in the fibre classifier as a function of different flow regimes. Total flow through the classifier was 5 l/min in each case. Radial position within the classifier is proportional to the square root of sample flow. (a) Inner sheath 1.75 l/min, outer sheath 1.75 l/min, inlet 1.5 l/min. (b) Inner sheath 0.58 l/min, outer sheath 3.92 l/min, inlet 0.5 l/min. (c) Inner sheath 3.92 l/min, outer sheath 0.58 l/min, inlet 0.5 l/min. (d) Inner sheath 2.25 l/min, outer sheath 2.25 l/min, inlet 0.5 l/min.

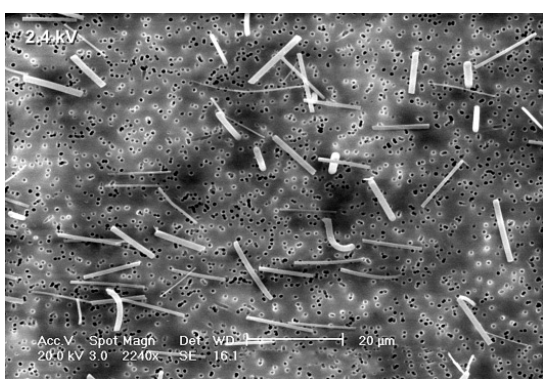


**Fig. 3.** Electron micrograph of classified fibres at an operating voltage of 2.4 kV.

parameters as a function of voltage and Fig. 5 shows length plotted against $1/V_{RMS}$. Mean fibre lengths were calculated with no pre-assumptions of length distribution. The relationship may be approximated by a linear function, as predicted from theory. The calibration function used was based on a least squares fit of $1/V_{RMS}$ against geometric fibre length, giving

$$\text{fibre length} = 33.267/V_{RMS} \quad (1)$$

where fibre length is in µm and $V_{RMS}$ is in kV.

## EXPERIMENTAL METHOD

Operating the classifier with an aerosol flow rate of 0.5 l/min led to a relatively low concentration of classified fibres. Where there were few fibres of a given length in the starting material (typically there were relatively few long fibres in the aerosolized powder) classified fibre concentrations could fall below 0.1 fibres/cm$^3$. Given the low particle concentrations achievable using the fibre classifier, fibre penetration through each thoracic sampler was measured by placing the sampler in-line with the classifier sample flow. As a result, only internal penetration efficiency was measured for each sampler, and not aspiration efficiency. However, it is unlikely that fibre length will have had a significant effect on aspiration efficiency with any of the samplers at the aerodynamic diameters used (Maynard, 1999).

Classified fibres from the classifier were passed either directly through a thoracic sampler or through a bypass line with similar flow characteristics (Fig. 6). A proportion of the aerosol was then sampled and sized using an APS. While it is not clear how the APS will have responded to the fibres, it was assumed that the instrument gave an accurate relative measurement of fibre concentration and that the reported aerodynamic diameter approximated that of the fibres analysed. To minimize the effect of fibre aerodynamic diameter on penetration measurements, only fibres

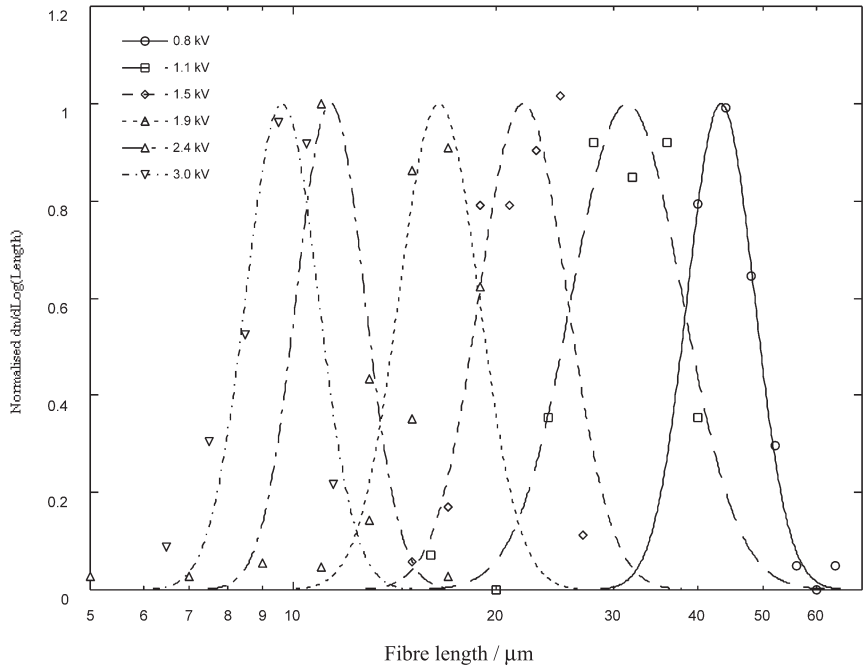


**Fig. 4.** Normalized fibre length distributions as a function of classifier voltage, showing measured distribution data (points) and fitted log normal functions (lines).

Table 1. Calibration data for the fibre classifier

| | $V_{RMS}$ (kV) | | | | | | |
|---|---|---|---|---|---|---|---|
| | 1.90 | 0.78 | 3.03 | 1.50 | 2.40 | 1.05 | 4.04 |
| $1/V_{RMS}$ ($kV^{-1}$) | 0.53 | 1.28 | 0.33 | 0.66 | 0.42 | 0.96 | 0.25 |
| Mean length (µm) | 16.55 | 45.43 | 9.51 | 22.09 | 12.06 | 31.45 | 7.25 |
| Geometric mean length (µm) | 16.51 | 45.07 | 9.45 | 21.91 | 11.85 | 30.98 | 7.10 |
| Predicted mean length (µm) | 16.58 | 40.31 | 10.37 | 20.91 | 13.11 | 30.06 | 7.79 |
| Predicted geometric mean length (µm) | 17.55 | 42.65 | 10.97 | 22.12 | 13.87 | 31.80 | 8.24 |

Predicted values are based on a linear function of the form length = $a/V_{RMS}$, with length in µm and $V_{RMS}$ in kV. $a$ = 31.44 for predicted mean length and $a$ = 33.27 for predicted geometric mean length.

with APS-measured aerodynamic diameters between 0.5 and 5 µm were counted for analysis purposes (approximate geometric diameters of 0.4–3.5 µm). Within this range, all samplers had previously been shown to have a penetration of ~100% (Maynard, 1999). In order to reconcile the classifier output flow rate, the thoracic sampler operating flow rate and the APS sampling flow rate, two flow loops were utilized. A re-circulating pump was used to remove flow $Q_2$ from the flow system after the sampler testing leg and return it to the classifier outlet flow prior to the sampler testing leg, thus providing the correct operating flow for the sampler ($Q_1$ + $Q_2$, where $Q_1$ is the classifier outlet flow). Likewise, the HEPA-filtered exhaust air from the APS was re-circulated prior to the point at which the APS sample was taken, enabling it to sample at 5 l/min without affecting operation of the classifier. Care was taken to ensure complete mixing at each point where additional flow was added to the flow train.

Penetration analysis was performed by selecting a specific fibre length with the classifier, then making alternative measurements of fibre number over a given period passing through the sampler and the bypass line. Prior to measurements commencing, the stability of the fibre number concentration was measured. Figure 7 shows a typical classifier output with time for 34 µm long fibres; similar trends were observed at other fibre lengths. Although temporal stability appears to be poor, short-term variations can be approximated by random variations superimposed on a linearly varying base rate. By counting the number of particles penetrating the sampler and the bypass line alternately over periods of the order of 30–150 s the effect of random fluctuations and linear changes in mean concentration were cancelled and

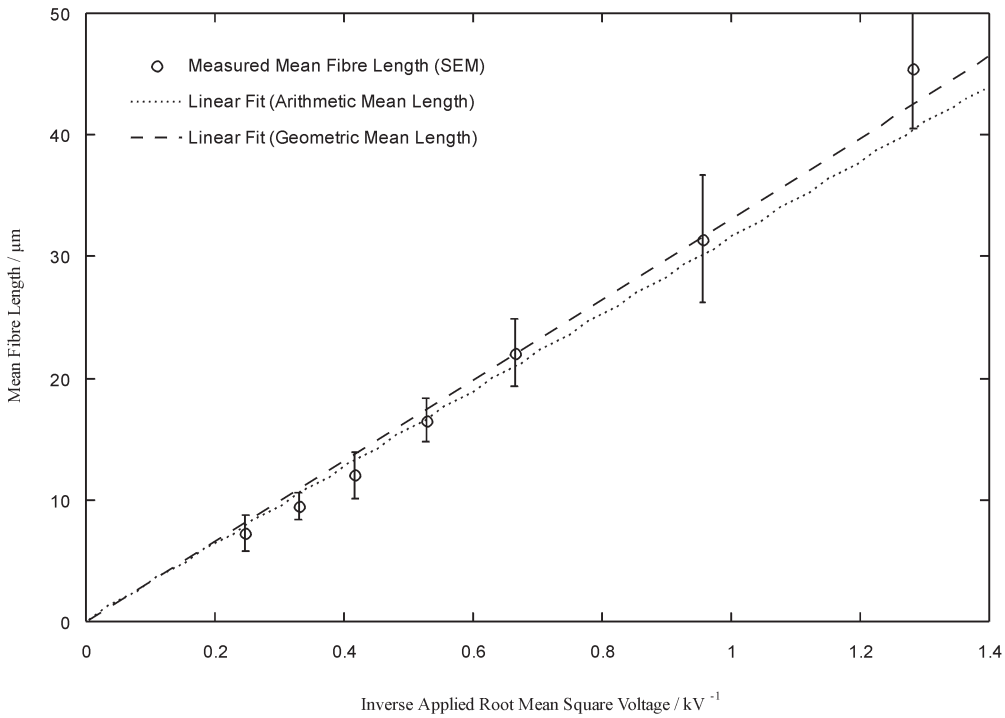


**Fig. 5.** Fibre classifier calibration as a function of inverse root mean square voltage. Inlet flow 0.5 l/min, sheath flows 2.25 l/min, sample flow 0.5 l/min.

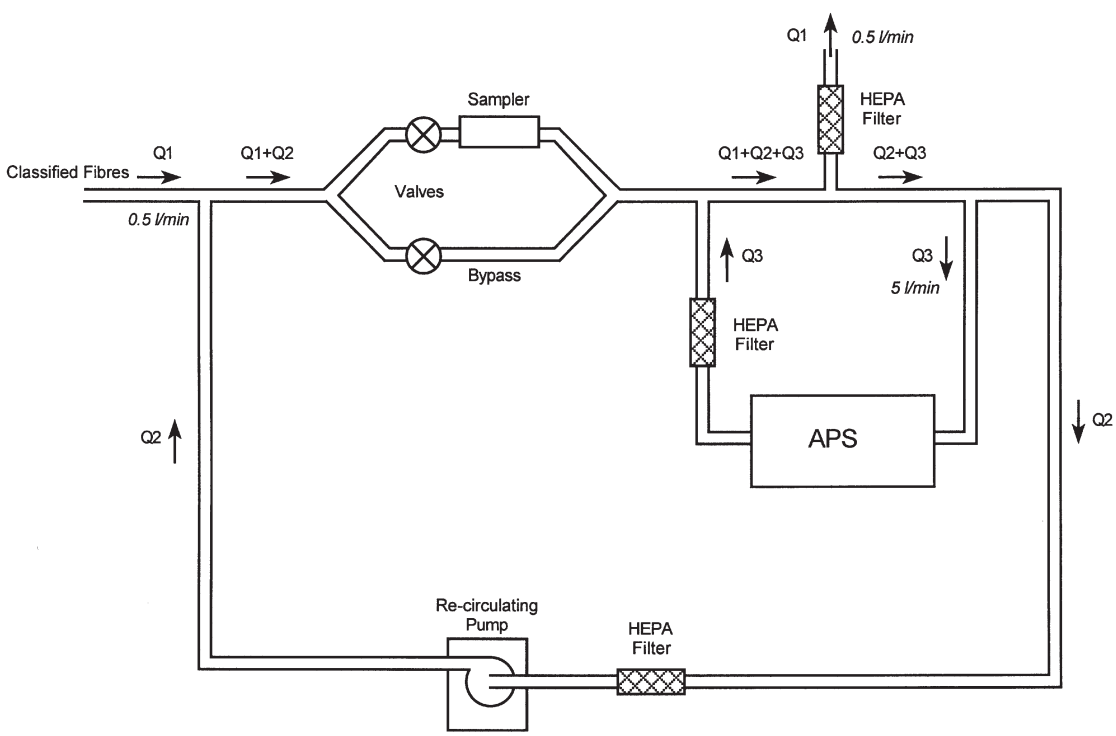


**Fig. 6.** Flow diagram of the sampler penetration measurement system. $Q_1$, output flow of the fibre classifier; $Q_1 + Q_2$, sampler flow; $Q_3$, APS sample flow. The flow system was designed to allow good aerosol mixing when additional airflow was introduced.

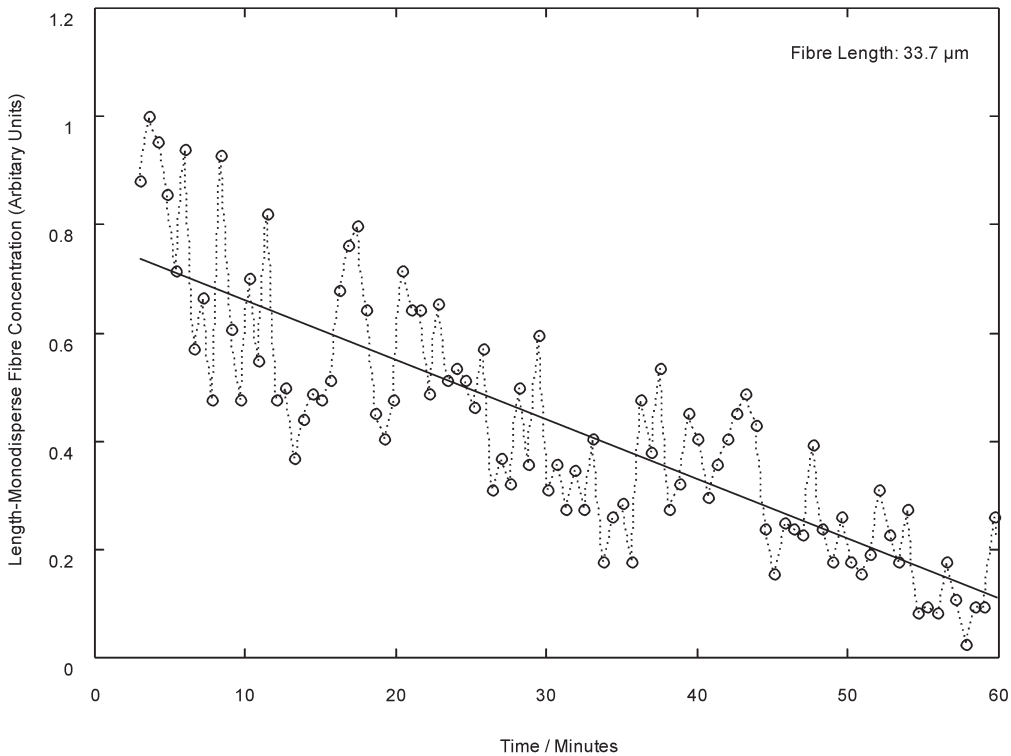


**Fig. 7.** Classifier output stability for 33.7 µm fibres, shown with a least squares linear fit to the data.

the influence of non-linear systematic variations minimized.

Each sampler was modified marginally to allow it to be placed in the test system without introducing leaks. The sampler outlets were attached to the system using the methods described by Maynard (1999). Fibrous aerosol was fed directly into the inlet of each sampler by inserting the sampler's inlet into tubing of an appropriate diameter. In the case of the CATHIA, the protective inlet cap was first removed. As experimental errors encountered were significantly greater than inter-sampler variability from compact particle tests (Maynard, 1999), only one of each sampler type was tested. Typically five fibre concentration measurements were made for each penetration measurement, with the first, third and fifth being through the thoracic sampler and the second and fourth through the bypass leg. Penetration was calculated by comparing average fibre concentrations passing through the sampler to the bypass line. For each fibre length a number of penetration measurements were made and the variance between measured values was used to estimate penetration measurement error.

## RESULTS AND DISCUSSION

Figures 8–12 show the measured penetration as a function of fibre length for each sampler type. Error bars are based on fibre count variability within each penetration measurement and represent ± 1 SD.

If fibre penetration was a function of aerodynamic diameter alone in each thoracic sampler, variations as a function of length would be small and penetration would be close to 100% at all lengths. Some deviation from 100% would be expected as, over the range of fibre aerodynamic diameters used, the penetration of some samplers has been measured to be less than 100% (Maynard, 1999). The extent of this deviation is dependent on the aerodynamic size distribution of the fibrous aerosol and the penetration function of the sampler. Variations in aerodynamic size distribution at differing classified lengths would be expected to lead to small length-dependent variations in penetration.

Below fibre lengths of 40 µm there are indications that the penetration through each sampler is marginally below 100% and that there is a dip in penetration around 20–30 µm. These features are most likely dominated by separation in terms of aerodynamic diameter and are not of concern. However, the degree to which there is some deviation from 100% penetration at small lengths varies more than would be expected between the different sampler types, with the modified SIMPEDS being closest to 100% (Fig. 8) and the CATHIA dropping to as low as 80% (Fig. 10). Previously measured penetration as a function of aerodynamic diameter does not explain these

Table 2. Non-linear regression on sampler penetration as a function of fibre length

| Sampler | $b$ | | $m$ | | $P\ (m = 0)$ |
|---|---|---|---|---|---|
| | Estimated value | Standard error | Estimated value | Standard error | |
| Modified SIMPEDS | 28.534 | 99.011 | 0.00143 | 0.00664 | 0.584 |
| IOM foam thoracic | 28.864 | 12.710 | –0.0125 | 0.0066 | 0.038 |
| CATHIA | –1432.5 | –8292.5 | –0.000103 | –0.000580 | 0.494 |
| GK 2.69 | –52.813 | 69.252 | –0.00136 | 0.00107 | 0.423 |
| Modified IOM inhalable | –28.747 | 22.952 | –0.00187 | 0.00065 | 0.583 |

Penetration has been modelled using equation (2). The final column gives the probability $P$ of $m = 0$, where $m$ is the rate of change of penetration with respect to fibre length for $l \geq b$.

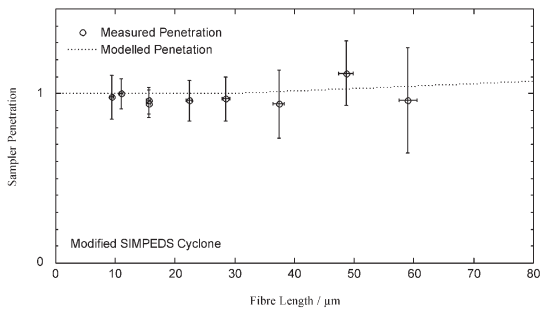


**Fig. 8.** Measured fibre penetration as a function of length through the modified SIMPEDS cyclone.

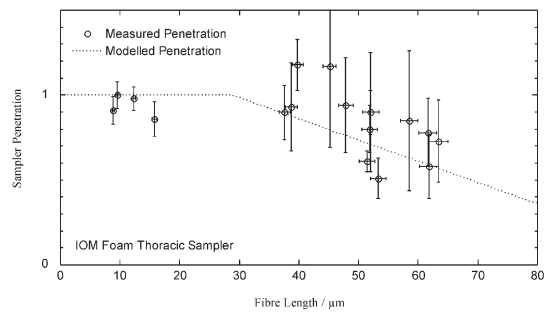


**Fig. 9.** Measured fibre penetration as a function of length through the IOM foam thoracic sampler.

features. In the case of the CATHIA sampler there was some evidence to suggest that the coupling method used between the flow system and the sampler contributed to some degree to the low penetration values. There were no other clear sources of the deviation identified during the investigation. However, the observed trend of the deviation from 100% penetration being an inverse function of sampler flow rate does suggest a systematic source of error linked to sampler flow.

For fibres longer than 40 µm no clear deviation from 100% penetration was observable in most of the samplers. However, given the magnitude of the experimental errors in this length range actual penetration could have been as low as 60% in some cases. The only sampler that appeared to show substantial deviation from 100% penetration was the IOM foam thoracic sampler (Fig. 9). A general trend was observed in this sampler with fibres longer than 50 µm of decreasing penetration with increasing fibre length.

Sampler performance may be quantitatively assessed by assuming penetration to be 100% below a given length $b$ and linearly decreasing with respect to fibre length above $b$, giving modelled penetration as

$$P_{\text{model}} = \begin{cases} 1, l < b \\ m(l-b)+1, l \geq b \end{cases} \quad (2)$$

where $l$ is fibre length and $m$ is the rate of change of penetration with $l > b$. Non-linear regression of penetration data against equation (2) leads to the values of $m$ and $b$ given in Table 2. Figures 8–12 also show modelled penetration. For each sampler the probability of $m = 0$ is also calculated. At a significance level of 95% only the IOM foam thoracic sampler shows a significant trend of decreasing penetration with increasing fibre length.

It is possible that the use of a polyurethane foam pre-separator in this sampler was responsible for the decrease in penetration at higher fibre lengths. Comparison with the modified IOM inhalable sampler shows no significant decrease in sampling efficiency with long fibres in the latter. However, the aerosol residence time within the modified IOM inhalable sampler was substantially less than in the IOM foam thoracic sampler. While these data are insufficient to indicate a possible length-dependent selection mechanism within the foam pre-separators, it is worth noting that fibre residence time close to deposition surfaces within these pre-separators is significantly longer than that in the other samplers included here. Under these conditions the contribution of length-dependent phoretic deposition mechanisms, such as dielectrophoresis, may become significant. Increased deposition due to fibre interception is unlikely in either of these samplers, as the mean pore size in each

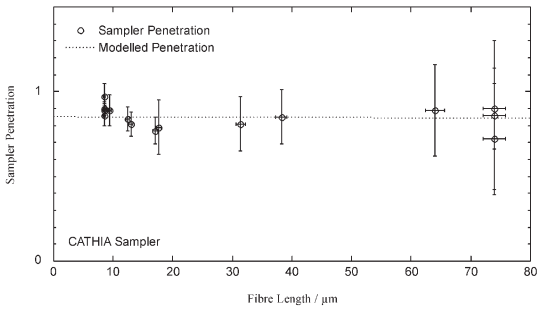


**Fig. 10.** Measured fibre penetration as a function of length through the CATHIA thoracic sampler.

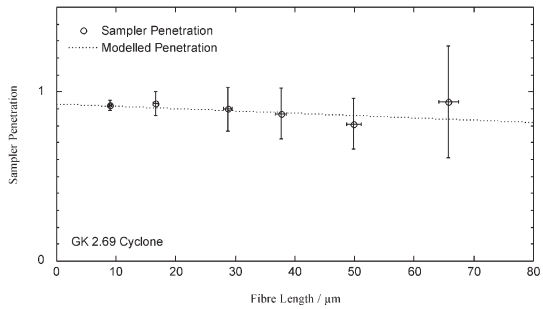


**Fig. 11.** Measured fibre penetration as a function of length through the GK2.69 cyclone.

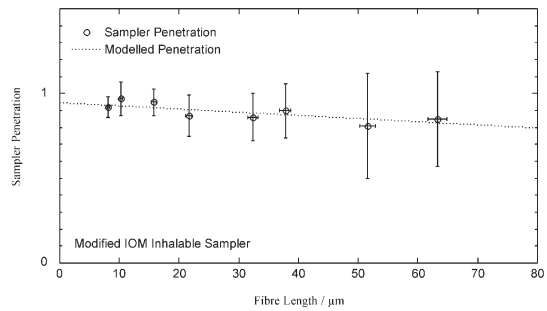


**Fig. 12.** Measured fibre penetration as a function of length through the modified IOM inhalable sampler.

case was an order of magnitude larger than the longest fibres used.

With the exception of the IOM foam thoracic sampler, the penetration measurements indicate that for fibres up to 60 µm long penetration efficiency is >60–80%. For all samplers, bar this one, the data do not indicate a trend of decreasing penetration with increasing length, thus supporting extrapolation of these findings to longer fibres. Compared with current inaccuracies in fibre sampling and counting, errors of this magnitude are relatively small and these measurements do not demonstrate the presence of detrimental length-dependent effects in the modified SIMPEDS cyclone, the CATHIA sampler, the GK2.69 cyclone or the IOM inhalable sampler with thoracic foam insert. However, use of the IOM foam thoracic sampler should be approached with caution.

Although these results pave the way to developing a size-selective fibre sampling protocol, there are a number of outstanding questions that need addressing before thoracic samplers take the place of the cowled samplers currently used. These include assessing the homogeneity of filter deposits from these samplers and comparison with current sampling methods in the field.

Some of these questions have been addressed by Jones *et al.* (2001) in a recent European collaborative study. The size-selective performance of a number of thoracic samplers (including those described here) was compared with that of cowled samplers in the laboratory using a length-polydisperse glass fibre aerosol in conjunction with size analysis in a SEM. Fibre penetration as a function of aerodynamic diameter agreed well with sampler performance when challenged with spherical particles in each case. There was an indication that the IOM foam thoracic sampler may have shown lower penetration efficiencies for fibres longer than 50 µm, in agreement with the present study. However, the imprecision associated with the analysis method prevented the significance of this perceived effect to be ascertained. Sampler comparisons in the field identified minimal differences between the thoracic and cowled samplers. There was evidence in some cases that the IOM foam thoracic sampler underestimated the fibre concentration, but this appeared to be associated with specific sites. These results generally appear to be in agreement with the findings presented here.

## CONCLUSIONS

The accuracy and precision of airborne fibre concentration measurements is notoriously poor and any potential improvement in the analysis method needs to be given careful consideration. By adopting size-selective sampling protocols, one of the potential sources of error, the presence of large compact particles, agglomerates and fibre clumps in samples, can be reduced or removed. The adoption of a suitable sampling convention also has the advantage of bringing fibre sampling in line with generic occupational aerosol sampling protocols. Although fibres currently considered harmful are those penetrating to the deep lung, respirable samplers will exclude some fibres presently considered harmful on aerodynamic grounds. The application of the thoracic sampling convention to fibres presents a pragmatic alternative in that it allows the collection of most fibres currently considered countable on aerodynamic grounds, but excludes large compact particles. However, it is possible that in some samplers pre-selection mechanisms other than inertial separation apply to fibres. Hence the need to characterize sampler performance

as a function of particle shape (in this case length) as well as aerodynamic diameter.

This investigation has provided penetration measurements as a function of fibre length for five thoracic samplers, using respirable fibres with lengths between 10 and 60 μm. Measurements on four of the samplers, the modified SIMPEDS cyclone, the GK2.69 cyclone, the CATHIA sampler and the IOM inhalable sampler with a foam insert, indicate no length-dependent sampling effects for fibres shorter than 60 μm. For these samplers extrapolation of the data indicates penetration is unlikely to be affected by fibre length at longer lengths. Penetration measurements on the IOM foam thoracic sampler indicate a trend of decreasing penetration with increasing fibre length above 30 μm. With the exception of the IOM foam thoracic sampler, the penetration measurements indicate that for fibres up to 60 μm long penetration efficiency is >60–80%. The use of any of these samplers for airborne fibre sampling is therefore unlikely to lead to significant deviation from current sampling protocols under ideal situations and will potentially lead to improved accuracy and precision where relatively high concentrations of large compact particles are experienced.

*Acknowledgements*—This work was made possible through the loan of equipment and support from Paul Baron and Gregory Deye at the National Institute for Occupational Safety and Health, Cincinnati, Ohio. The research was supported by the UK Health & Safety Executive.

## REFERENCES

Aitken R, Vincent J, Mark D. (1993) Applications of porous foams as size selectors for biologically relevant samplers. Appl Occup Environ Hyg; 8: 363–9.

American Conference of Government Industrial Hygienists. (1998) Particle size-selective sampling for particulate air contaminants. Cincinnati, OH: American Conference of Government Industrial Hygienists.

Baron PA. (1996) Application of the thoracic sampling definition to fiber measurement. Am Ind Hyg Assoc J; 57: 820–4.

Baron PA, Deye GJ, Fernback J. (1994) Length separation of fibers. Aerosol Sci Technol; 21: 179–92.

Baron PA, Deye GJ, Fernback JE, Jones WG. (1998) Direct-reading measurement of fiber length/diameter distributions. In Advances in Environmental Measurement Methods for Asbestos. Boulder, CO: American Society for Testing Materials.

Chen BT, Irwin R, Cheng YS, Hoover MD, Yeh HC. (1993) Aerodynamic behaviour of fibre- and disc-like particles in a Millikan cell apparatus. J Aerosol Sci; 24: 181–95.

Comité Européen de Normalisation. (1993) Workplace atmospheres—size fraction determination for measurement of airborne particles, EN 481. Brussels: Comité Européen de Normalisation.

Deye GJ, Gao P, Baron PA, Fernback J. (1999) Performance evaluation of a fiber length classifier. Aerosol Sci Technol; 30: 420–37.

Fabriès JF, Görner P, Kauffer E, Wrobel R, Vigneron JC. (1998) Personal thoracic CIP10-T sampler and its static version CATHIA-T. Ann Occup Hyg; 42: 453–65.

International Standards Organization. (1995) Air quality—particle size fraction definitions for health-related sampling, ISO standard 7708. Geneva: International Standards Organization.

Jones AD, Aitken RJ, Armbruster L *et al*. (2001) Thoracic sampling of fibres. Norwich: HSE Books.

Kaye PH, Michelu F, Tracey MC, Hirst E, Gundlach AM. (1992) The production of precision silicon micromachined non-spherical particles for aerosol studies. J Aerosol Sci; 23 (suppl. 1): S201–4.

Kenny LC, Gussman RA. (1997) Characterization and modelling of a family of cyclone aerosol preseparators. J Aerosol Sci; 28: 677–88.

Kenny LC, Stancliffe JD. (1997) Design and optimisation of size-selective samplers based on porous foams, 11th Annual Conference of the Aerosol Society, Warwick, UK.

Lipowicz PJ, Yeh HC. (1989) Fiber dielectrophoresis. Aerosol Sci Technol; 11: 206–12.

Lippmann M. (1994a) Nature of exposure to chrysotile. Ann Occup Hyg; 38: 459–67.

Lippmann M. (1994b) Workshop on the health risks associated with chrysotile asbestos: a brief review. Ann Occup Hyg; 38: 638–42.

Maynard AD. (1999) Measurement of aerosol penetration through six personal thoracic samplers under calm air conditions. J Aerosol Sci; 30: 1227–42.

Vincent JH, Aitken RA, Mark D. (1993) Porous plastic foam filtration media: penetration characteristics and applications in particle size-selective sampling. J Aerosol Sci; 24: 929.

World Health Organization. (1997) Determination of airborne fibre number concentrations: a recommended method, by phase contrast optical microscopy (membrane filter method). Geneva: World Health Organization.